



# Enable Touch-based Communication between Laptop and Smartwatch

Dian Ding

dingdian94@sjtu.edu.cn  
Shanghai Jiao Tong University  
Shanghai, China

Yu Lu

yulu01@sjtu.edu.cn  
Shanghai Jiao Tong University  
Shanghai, China

Yijie Li

yijieli@sjtu.edu.cn  
Shanghai Jiao Tong University  
Shanghai, China

Yi-Chao Chen

yichao@sjtu.edu.cn  
Shanghai Jiao Tong University  
Shanghai, China

Hao Pan

panhao@microsoft.com  
Microsoft Research Asia  
Shanghai, China

Guangtao Xue

gt\_xue@sjtu.edu.cn  
Shanghai Jiao Tong University  
Shanghai, China

## ABSTRACT

Wearable devices, including smartwatches, are increasingly popular among consumers due to their user-friendly services. However, transmitting sensitive data like social media messages and payment QR codes via commonly used low-power Bluetooth exposes users to privacy breaches and financial losses. This study introduces *TouchHBC*, a secure and reliable communication scheme leveraging a smartwatch's built-in electrodes. This system establishes a touch-based human communication system utilizing a laptop's leakage current. As the transmitting device, the laptop modulates this current via the CPU. Simultaneously, the smartwatch, equipped with built-in electrodes, captures the current traversing the human body and decodes it. The modulation and decoding processes involve techniques such as amplitude modulation, spectral subtraction, channel estimation, and retransmission mechanisms. *TouchHBC* facilitates communication between laptops and smartwatches. Real-world tests demonstrate that our prototype achieves a throughput of 19.83bps. Moreover, *TouchHBC* offers the potential for enhanced interaction, including improved gaming experiences through vibration feedback and secure touch login for smartwatch applications by synchronizing with a laptop.

## CCS CONCEPTS

- Human-centered computing → Ubiquitous and mobile devices.

## KEYWORDS

Human Body Communication, Leakage Current, Laptop, Smart Watch

### ACM Reference Format:

Dian Ding, Yijie Li, Hao Pan, Yu Lu, Yi-Chao Chen, and Guangtao Xue. 2024. Enable Touch-based Communication between Laptop and Smartwatch. In *Companion of the 2024 ACM International Joint Conference on Pervasive and Ubiquitous Computing (UbiComp Companion '24)*, October 5–9, 2024,

Permission to make digital or hard copies of all or part of this work for personal or classroom use is granted without fee provided that copies are not made or distributed for profit or commercial advantage and that copies bear this notice and the full citation on the first page. Copyrights for third-party components of this work must be honored. For all other uses, contact the owner/author(s).

*UbiComp Companion '24*, October 5–9, 2024, Melbourne, VIC, Australia

© 2024 Copyright held by the owner/author(s).

ACM ISBN 979-8-4007-1058-2/24/10

<https://doi.org/10.1145/3675094.3677574>

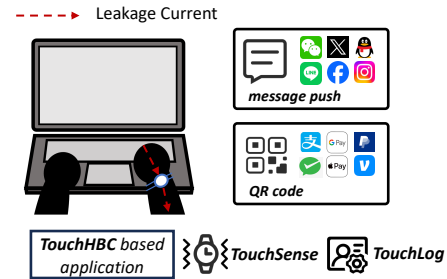


Figure 1: Human body communication of *TouchHBC*.

Melbourne, VIC, Australia. ACM, New York, NY, USA, 5 pages. <https://doi.org/10.1145/3675094.3677574>

## 1 INTRODUCTION

Smartwatches, renowned for user-friendly services like health monitoring and sports management, saw global spending reach 31.3 billion in 2022 [12]. However, these devices predominantly rely on limited communication methods, with low-power Bluetooth being the most common. This protocol is vulnerable as attackers can simulate low-volume devices to circumvent its encryption and authentication processes, potentially leading to information theft [18]. Although some models support cellular networks, they tend to be more costly.

Unlike devices such as smartphones, smartwatches typically receive smaller texts, such as prompting messages from social software logged into other devices. In addition, with the growing popularity of mobile payments, smartwatches can synchronize QR codes from payment software for transactions. While these transmissions do not demand high communication rates, communication security is critical. Information leakage will bring non-negligible risks to the user's financial security and personal privacy.

This paper focuses on **developing a secure and efficient communication system utilizing smartwatch's inherent components**. Based on this, we propose a new smartwatch communication solution, *TouchHBC*, facilitating a touch-based human body communication system using the leakage current of a laptop. As shown in Fig. 1, a user simply needs to touch the metal casing of the laptop with his hand, enabling the smartwatch's built-in electrodes to capture the leakage current flowing through the human body.

This system can synchronize social media messages, and authenticate information like accounts, passwords, and payment QR codes without hindering the laptop's normal functions.

The leakage current, serving as the communication medium, originates from a safety capacitor in the laptop's adapter [5, 7] and varies with the laptop's operation [3, 10]. By modulating high-consumption components of the laptop such as the CPU, the system can modulate the spectral characteristics of the leakage current for data transmission.

In this study, we introduce a touch-based human body communication system *TouchHBC* that consists of two components: a transmitter and a receiver. The transmitter modulates the leakage current through the power consumption of the laptop CPU and employs a retransmission mechanism to improve the reliability of the communication. The receiver consists of leakage current pre-processing and decoding.

## 2 RELATED WORKS

Recent researchers have developed numerous communication methods using various media to establish different communication systems based on bypass signals.

**2.0.1 Acoustic Communication.** MUDIS [9] enabled multi-user audible acoustic directional communication based on the parametric array and acoustic metasurface. Endophasia [21] implemented silent speech commands on the smartphone using GSM signals. MagicInput [14] achieved handwriting recognition based on 1-dimensional tracking using acoustic signals.

**2.0.2 Magnetic Communication.** MagneComm [13, 20] regulated the magnetic induction signal from the CPU and enabled near-field communication via magnetometer sensing on the device. MagView [21] achieved magnetic communication by changing the video packet type and reducing the quantization parameter to effectively control the CPU utilization of video decoding.

**2.0.3 Vibration Communication.** Ripple [15] explored the possibility of using physical vibrations as a mode of wireless communication. VibWriter [4, 6] used the built-in accelerometer of the smartphone to identify the handwriting on the same table.

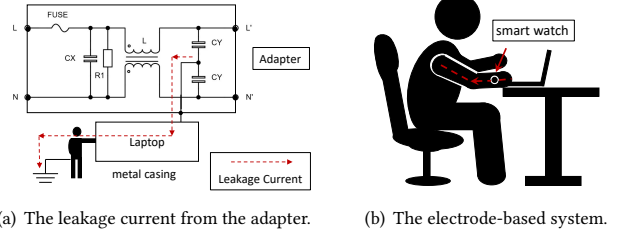
## 3 BACKGROUND

### 3.1 Leakage Current

As a laptop with a metal casing (such as a MacBook) is connected to a power source, the metal casing of the laptop carries the leakage current from the adapter [7]. The leakage current comes from the Y-capacitor (safety capacitor) of the adapter and is usually configured on both the high and low-voltage sides of the SMPS. As a common mode capacitor, grounding of the Y capacitor generates the leakage current [5, 19]:

$$I = 2\pi f C_h U_h + k C_l U_l + I_{cmi} \quad (1)$$

where the leakage current in the high voltage side is  $2\pi f C_h U_h$ ,  $f$  refers to the mains frequency,  $C_h$  indicates the size of the capacitor, and  $U_h$  indicates the voltage. On the low-voltage side,  $k$  is the leakage current constant (about 0.01 to 0.03 depending on the manufacturer),  $C_l$  and  $U_l$  denote the corresponding Y capacitor



(a) The leakage current from the adapter.

(b) The electrode-based system.

Figure 2: Fundamental principle of leakage current.

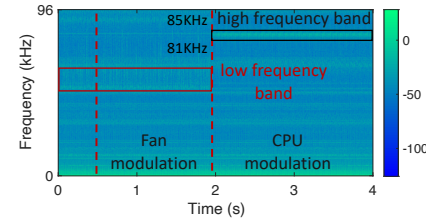


Figure 3: Leakage current as CPU power consumption increases.

and voltage. The Y capacitors used in laptop adapters are typically around  $5nF$ .  $I_{cmi}$  represents the common mode interference (high-frequency harmonics) in the SMPS and contains a disturbance signal generated by the fluctuations of loading states [10], such as the high computing rate of the CPU. Therefore, a laptop powered by the  $220V/50Hz$  mains generates roughly  $0.3mA$  of leakage current at the casing ( $U_l = 12V$ ).

### 3.2 Feasibility of TouchHBC

When using the laptop naturally, the user's hand is placed on the laptop in contact with the metal casing, and the feet are placed on the ground. The leakage current flows from the laptop through the human body and eventually into the ground, as shown in Fig. 2(a). The electrodes on the skin can perceive weak current flowing through the human body [11, 16, 17]. We therefore use the built-in electrode of the smartwatch to capture the leakage current (Fig. 2(b)).

As the leakage current is related to the working state of the laptop [10], we modulated the fan and CPU separately. The leakage currents collected by the built-in electrode are shown in Fig. 3, we calculated the spectrogram of the leakage current using Short-Time Fourier Transform (STFT). It can be seen that the leakage current is significantly enhanced when modulating the CPU to high power consumption. Furthermore, the CPU can be easily controlled by *loop* and *sleep* commands, which are available for most programming languages and operating systems.

It can be seen that the signal in the high-frequency band (black box in Fig. 3) of the leakage current is significantly increased (concentrated between  $82KHZ$  and  $84KHz$ ) when the CPU is at high power consumption. There is a corresponding attenuation of the signal in the low-frequency band (red box in Fig. 3).

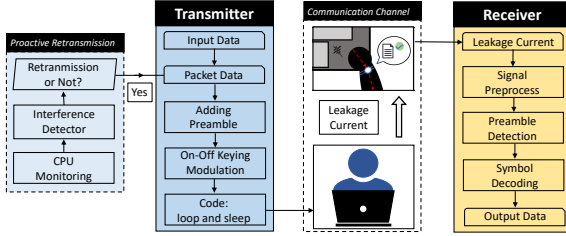


**Figure 4: System architecture of the *TouchHBC* system.**

## 4 SYSTEM

### 4.1 Transmitter Design

**4.1.1 Preamble.** *TouchHBC* sets a unique pattern of the leakage current for the preamble at the start of each data packet so that the system can use cross-correlation to locate the start time of the transmission. Moreover, the system can perform an initial estimation of the channel using the preamble.

**4.1.2 Modulation.** We chose On-Off Keying for the modulation of the data bits. The choice of transmission rate depends on the precision of the leakage current control. The control precision is defined as  $P_{control} = \frac{1}{n} \sum_{i=1}^n (U_{real,i} - U_{desired,i})^2$ , where  $U_{desired}$  is the desired leakage current amplitude and  $U_{real}$  is the actual amplitude. We test the control accuracy of the electrode-based system at different transmission rates and a lower value for  $P_{control}$  means that we can control the leakage current more precisely.

**4.1.3 Proactive Retransmission.** After a data packet has been sent, we determine whether there is interference during transmission by monitoring the CPU. If the usage of two or more non-transmitter CPU cores exceeds 30%, the transmitter will determine that there is interference with the symbol currently being sent. The transmitter will re-transmit the entire data packet if there is a corrupted symbol in the packet.

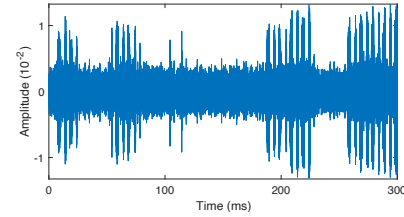
### 4.2 Receiver Design

**4.2.1 Signal Preprocessing.** The modulation of leakage current with the CPU is mainly reflected in specific frequency bands, as shown in Fig. 3. Therefore, we use a band-pass filter to extract the signal in this band of the leakage current. Considering the noise present in the leakage current, we denoise the signal using spectral subtraction [8] based on the noise samples taken at idle moments as follows:

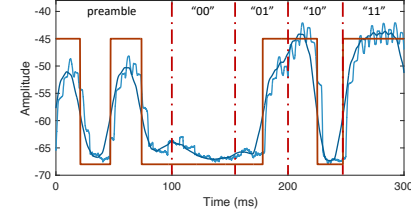
$$\|Y(k)\|^2 = \|S(k)\|^2 - \alpha \|N(k)\|^2 \quad (2)$$

where  $k$  represents the frequency range of the band,  $S(k)$  and  $N(k)$  represent filtered signal and noise signal respectively.  $\alpha$  is the ratio of the signal strength of each frequency corresponding to symbol 0 in the current channel to the signal strength of the noise sample. To reduce the effect of signal fluctuations, we set a processing window of 0.02s and calculate the logarithmic short-time energy (log-STE) of the processing window as follows:

$$E(j) = 10 \log \sum_{i=j}^{j+0.02 \times F_s} y(i)^2 \quad (3)$$



(a) Modulate the leakage current with the preamble and the binary sequence.



(b) Preprocess and decode the leakage current.

**Figure 5: Transmission example:** Fig. 5(a) Modulate the leakage current at the transmitter; Fig. 5(b) Preprocess and decode the leakage current at the receiver.

where  $y(i)$  represents the leakage current signal and  $F_s$  represents the sampling rate of the receiver. To further smooth out the fluctuations in the signal, the signal was processed with a mean window of 0.02s in duration.

**4.2.2 Signal Decoding.** After pre-processing, we can identify the symbols corresponding to different signal segments. We detect the preamble to synchronize the transmitter and receiver and calculate the signal amplitude corresponding to different symbols. Then, we validated the system by two-bit binary coding. We added the preamble at the beginning of the example and modulated the leakage current for communication. The received leakage current is shown in Fig. 5(a), and the leakage current is preprocessed and decoded as shown in Fig. 5(b).

## 5 EVALUATION

### 5.1 Evaluational Setup

The prototype of *TouchHBC* is adopted on a laptop (MacBook Pro) as a transmitter as shown in Fig. 6. The laptop is placed on the desk and kept in charge. We collected the leakage current using the built-in electrodes of the smartwatch (Apple Watch S6), which is worn on the left wrist, as shown in Fig. 6. Due to sensor permission issues, we used the AD2 [1] to collect data. The user can communicate with the smartwatch by touching the metal casing of the laptop.

### 5.2 Micro Benchmark

**5.2.1 Sampling Rate.** In the feasibility experiment, the sampling rate of the AD2 was set to 192KHz and we were able to use the leakage current of the laptop for communication. We seek to sample the leakage current based on the aliasing effect [2], thus reducing the limitation of the sampling rate. In this experiment, we evaluate the throughput and signal-to-noise ratio of *TouchHBC* in two environments at various sampling rates from 48KHz to 192KHz. We

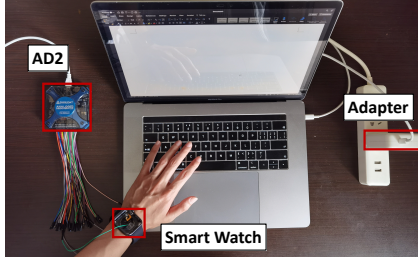


**Figure 6: Evaluational Setup of the TouchHBC system.**

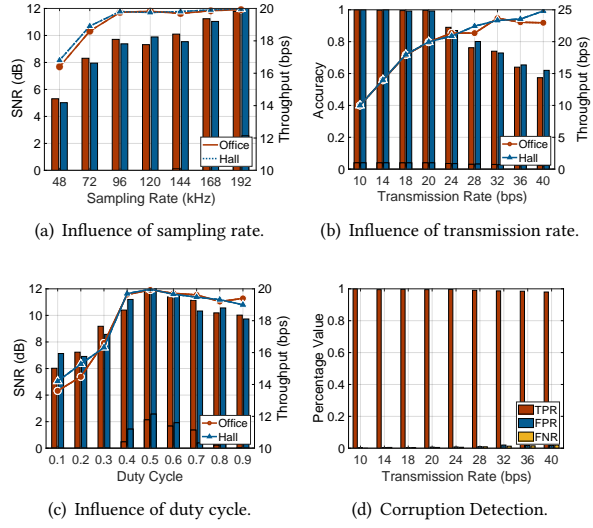


**Figure 7: Evaluation of the TouchHBC system.**

keep the transmission rate and duty cycle as  $20\text{bps}$  and  $0.5$ , and the performance of the system is shown in Fig. 7(a).

**5.2.2 Transmission Rate.** We adjust the transmission rate of the leakage current to test the transmission rate of the system. We increased the transmission rate from  $10\text{bps}$  to  $40\text{bps}$  and measured the accuracy and throughput of the communication. As shown in Fig. 7(b), the transmission rate is increased from  $10\text{bps}$  to  $20\text{bps}$  and the communication accuracy remains above  $99.1\%$ . When the transmission rate is higher than  $20\text{bps}$ , the communication accuracy decreases significantly, and the low accuracy may seriously affect the reliability of the communication system.

**5.2.3 Duty Cycle.** We increase the duty cycle from  $0.1$  to  $0.9$  and keep the sampling rate and transmission rate at  $192\text{KHz}$  and  $20\text{bps}$  in the process. As shown in Fig. 7(c), with a duty cycle of  $0.5$ , the system can achieve the maximum throughput and SNR. As the duty cycle increases or decreases, both throughput and SNR decrease, especially as the duty cycle decreases.

**5.2.4 Corruption Detection.** To further guarantee the reliability of TouchHBC, one-way communication requires the transmitter to accurately detect and retransmit the data bits. We increased the transmission rate from  $10\text{bps}$  to  $40\text{bps}$ , the results are shown in Fig. 7(d). At transmission rates below  $20\text{bps}$ , the TPR is  $99.5\%$  or higher, while the FNR is  $0.05\%$  or lower, indicating that our

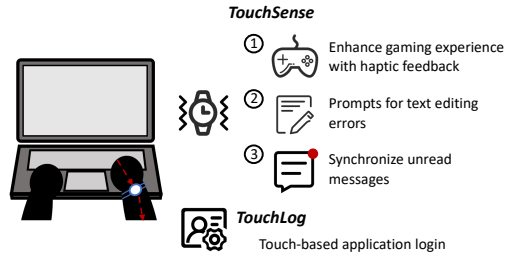


**Figure 8: Extended applications of TouchHBC.**

corruption detection algorithm on the transmitter can correctly detect corrupted symbols.

## 6 APPLICATION

### 6.1 TouchSense

Vibration feedback is now widely used in smartphones, switch consoles, and other devices to provide more realistic and interesting interactions while playing games. However, it is difficult for laptops to provide electronic components such as motors for vibration feedback. With the built-in motors in smartwatches, we can expand smartwatches into vibration feedback modules for laptops.

The smartwatch can extract the data embedded in the leakage current and define different vibration methods to achieve different feedback. As shown in Fig. 8, TouchSense can achieve real vibration feedback in the process of playing games, prompting typos during text editing, as well as prompting messages without affecting the screen display when watching videos on full screen.

### 6.2 TouchLog

As the hardware performance of smartwatches improves, the types of services they support and the number of apps they offer show explosive growth. It is difficult for users to directly manage the numerous accounts and passwords, and these may contain private information such as payment software and social software. Inspired by the Chrome browser to manage accounts and passwords for multiple websites, we can use a laptop to manage account passwords for different APPs in smartwatches and embed the information into leakage currents to log into different APPs in smartwatches and transmit information such as payment QR codes.

## 7 CONCLUSION

In this paper, we build a touch-based human communication system using the built-in electrodes of a smartwatch. The proposed system embeds information into the leakage current of a laptop to achieve communication. TouchHBC implements the communication between a laptop and a smartwatch with a throughput of  $19.83\text{bps}$ . Furthermore, rich interaction extensions such as vibration feedback, account management, etc. can be implemented on smartwatches based on the proposed system.

## ACKNOWLEDGMENTS

This work is supported in part by the NSFC (61936015,62072306).

## REFERENCES

- [1] DIGILENT AD2. 2021. <https://digilent.com/shop/analog-discovery-2-100ms-s-usb-oscilloscope-logic-analyzer-and-variable-power-supply/>
- [2] Yuchi Chen, Wei Gong, Jiangchuan Liu, and Yong Cui. 2017. Fine-grained ultrasound range finding for mobile devices: Sensing way beyond the 24 kHz limit of built-in microphones. In *IEEE INFOCOM*. 845–850. <https://doi.org/10.1109/INFCOMW.2017.8116486>
- [3] Dian Ding, Yi-Chao Chen, Xiaoyu Ji, and Guangtao Xue. 2023. LeakThief: Stealing the Behavior Information of Laptop via Leakage Current. In *2023 20th Annual IEEE International Conference on Sensing, Communication, and Networking (SECON)*. 186–194. <https://doi.org/10.1109/SECON58729.2023.10287495>
- [4] Dian Ding, Lanqing Yang, Yi-Chao Chen, and Guangtao Xue. 2021. VibWriter: Handwriting Recognition System based on Vibration Signal. In *IEEE SECON*. 1–9. <https://doi.org/10.1109/SECON52354.2021.9491615>
- [5] Dian Ding, Lanqing Yang, Yi-Chao Chen, and Guangtao Xue. 2022. Leakage or Identification: Behavior-Irrelevant User Identification Leveraging Leakage Current on Laptops. *PACM IMWUT* 5, 4, Article 152 (dec 2022), 23 pages. <https://doi.org/10.1145/3494984>
- [6] Dian Ding, Lanqing Yang, Yi-Chao Chen, and Guangtao Xue. 2023. Handwriting Recognition System Leveraging Vibration Signal on Smartphones. *IEEE Transactions on Mobile Computing* 22, 7 (2023), 3940–3951. <https://doi.org/10.1109/TMC.2022.3148172>
- [7] Milind M. Jha, Kunj Behari Naik, and Shyama Prasad Das. 2009. Estimation of Optimum Value of Y-Capacitor for Reducing Emi in Switch Mode Power Supplies. *Electrical Power Quality and Utilisation. Journal* (2009).
- [8] S. Kamath and P. Loizou. 2002. A multi-band spectral subtraction method for enhancing speech corrupted by colored noise. In *2002 IEEE International Conference on Acoustics, Speech, and Signal Processing*, Vol. 4. IV-4164–IV-4164. <https://doi.org/10.1109/ICASSP.2002.5745591>
- [9] Yijie Li, Juntao Zhou, Dian Ding, Yi-Chao Chen, Lili Qiu, Jiadi Yu, and Guangtao Xue. 2024. MuDiS: An Audio-independent, Wide-angle, and Leak-free Multi-directional Speaker. In *Proceedings of the 30th Annual International Conference on Mobile Computing and Networking* (Washington D.C., DC, USA) (*ACM MobiCom '24*). Association for Computing Machinery, New York, NY, USA, 263–278. <https://doi.org/10.1145/3636534.3649360>
- [10] William Meng. 2011. Touch current analysis for power supplies designed for energy efficient regulations. In *2011 IEEE Symposium on Product Compliance Engineering Proceedings*. 1–6. <https://doi.org/10.1109/PSES.2011.6088240>
- [11] Viet Nguyen, Mohamed Ibrahim, Hoang Truong, Phuc Nguyen, Marco Gruteser, Richard Howard, and Tam Vu. [n. d.]. Body-Guided Communications: A Low-Power, Highly-Confining Primitive to Track and Secure Every Touch (*MobiCom '18*). New York, NY, USA, 353–368. <https://doi.org/10.1145/3241539.3241550>
- [12] Gartner Forecasts Global Spending on Wearable Devices to Total 81.5 Billion in 2021. 2021. <https://www.gartner.com/en/newsroom/press-releases/2021-01-11-gartner-forecasts-global-spending-on-wearable-devices-to-total-81-5-billion-in-2021>
- [13] Hao Pan, Yi-Chao Chen, Guangtao Xue, and Xiaoyu Ji. [n. d.]. MagneComm: Magnetometer-Based Near-Field Communication (*ACM MobiCom '17*). 167–179. <https://doi.org/10.1145/3117811.3117824>
- [14] Hao Pan, Yi-Chao Chen, Qi Ye, and Guangtao Xue. [n. d.]. MagicInput: Training-Free Multi-Lingual Finger Input System Using Data Augmentation Based on MNISTs (*IPSN '21*). 119–131. <https://doi.org/10.1145/3412382.3458261>
- [15] Nirupam Roy and Romit Roy Choudhury. 2016. Ripple II: Faster Communication through Physical Vibration. In *USENIX NSDI*. 671–684.
- [16] Virag Varga, Gergely Vakulya, Alanson Sample, and Thomas R. Gross. 2018. Enabling Interactive Infrastructure with Body Channel Communication. *Proc. ACM Interact. Mob. Wearable Ubiquitous Technol.* 1, 4, Article 169 (Jan. 2018), 29 pages. <https://doi.org/10.1145/3161180>
- [17] Virag Varga, Marc Wyss, Gergely Vakulya, Alanson Sample, and Thomas R. Gross. 2018. Designing Groundless Body Channel Communication Systems: Performance and Implications (*UIST '18*). New York, NY, USA, 683–695. <https://doi.org/10.1145/3242587.3242622>
- [18] Jiliang Wang, Feng Hu, Ye Zhou, Yunhao Liu, Hanyi Zhang, and Zhe Liu. 2020. BlueDoor: Breaking the Secure Information Flow via BLE Vulnerability. In *Proceedings of the 18th International Conference on Mobile Systems, Applications, and Services* (Toronto, Ontario, Canada) (*MobiSys '20*). Association for Computing Machinery, New York, NY, USA, 286–298. <https://doi.org/10.1145/3386901.3389025>
- [19] S. Westerlund and L. Ekstam. 1994. Capacitor theory. *IEEE Transactions on Dielectrics and Electrical Insulation* 1, 5 (1994), 826–839. <https://doi.org/10.1109/94.326654>
- [20] Guangtao Xue, Hao Pan, Yi-Chao Chen, Xiaoyu Ji, and Jiadi Yu. 2021. MagneComm+: Near-Field Electromagnetic Induction Communication with Magnetometer. *IEEE Transactions on Mobile Computing* (2021), 1–1. <https://doi.org/10.1109/TMC.2021.3133481>
- [21] Juchuan Zhang, Xiaoyu Ji, Wenyuan Xu, Yi-Chao Chen, Yuting Tang, and Gang Qu. 2020. MagView: A Distributed Magnetic Covert Channel via Video Encoding and Decoding. In *IEEE INFOCOM 2020*. 357–366. <https://doi.org/10.1109/INFCOM41043.2020.9155386>